

### Sensitivity Analysis of Kinetic Growth Model Data: Monod Equation

**Abdulhalim Musa Abubakar**

Department of Chemical Engineering, Faculty of Engineering, Modibbo Adama University, Yola, Adamawa State, Nigeria

**Zahra Soltanifar**

Department of Fisheries, College of Agriculture and Natural Resources, University of Tehran, Enghelab Square, 16 Azar Street, Iran

**Mahlon Marvin Kida, Zidani Danladi Ahmed**

Department of Chemical Engineering, Faculty of Engineering, University of Maiduguri, Bama Road, Maiduguri, Borno State, Nigeria

#### Article Information

**Received:** October 13, 2022

**Accepted:** October 22, 2022

**Published:** October 28, 2022

**Keywords:** Sensitivity analysis; Monod; Growth kinetics; Substrate concentration; Cell concentration

#### ABSTRACT

*Simulation modeling of microbial proliferation had increased in recent years using Monod and advanced kinetic models. Accurate data is limited to advance studies in cell utilization for various applications due to complexity of the process. In this reasearch, behaviour of the Monod parameters at different substrate and biomass levels will be examined using predicted data obtained originally from empirical observations. Method involves deliberate variation of some variables to examine its effects on others starting from the basic Malthus equation. Results shows that, predicted data are more convinient and clearly presents the supposed dynamics of the process compared to ideal experimental results. By implications, improved procedures are necessary to allow for precise estimates of basic cell numbers and substrate concentration values.*

#### Introduction

The Monod model is the most basic kinetic equation for analysing the specific growth rate of microorganisms under favourable conditions. Different microorganisms require different environment to grow in size, produce new cells and survive. The surface on which microorganisms carryout these fundamental task is known as a substrate which include hydrogen peroxide and glucose, to mention a few, at neutral or acidic pH and mesophilic, psychrophilic, thermophilic or hydrothermophilic temperatures in susbtrates of high carbon proportion. Microbiologist and bioengineers had therefore tried to study conditions that favour the growth of hundreds of microorganisms to study their kinetics. This study is however carried out in three ways, namely batch, fed-batch and continuous culture in bioreactors and chemostats to generate cell and substrate concentration data. In bioengineering or biotechnological research, empirical growth data usually reported are different and is caused by changing cell adaptation to specific environment, presence of multiple microbial cells in a particular substrate, unrealistic cell

counting device and difficulty in maintaining conditions of reactor types that harbour them, makes them incomparable. However, when this experimental data are used to predict new ones by estimating certain kinetic parameters, these new correlated data happens to be too perfect. It is so, very suitable to work with these predicted data for substrate sensitivity studies especially using the combined Malthus and Monod equations. It is wrong to use Micheles-Menten equation for cell growth analysis as it is used mostly for process involving a single enzymes, while Monod is used for cells, as they are capable of generating more enzymes and substrate. Example is the fungus called yeast which produces maltase that breaks down maltose to glucose. Objectives of this work is to use an existitng predicted data of cell centration, X (mg/l) and substrate concentration, S (mg/l) at constant and varying conditions of the initial susbtrate concentrations,  $S_0$  to examine data flexibility. Nikitina & Chernukha (2020) had used the 1-step Runge-Kutta technique to solve differential equations in S and X by writing an R programming code in the Jupyter Notebook environment.

## Methodology

### Substrate Concentration

When the growth phase equation (1) (Rezvani et al., 2017) and the Malthus equation (2) (Sakthiselvan et al., 2019) are combined, the rate constant (k), equivalent to the maximum specific growth rate ( $\mu_{max}$ ) can be predicted using statistical data resulting in the predicted values of X.

$$\frac{dX}{dt} = \mu X \quad (1)$$

$$\mu = k \left( 1 - \frac{X}{X_{max}} \right) \quad (2)$$

Where,  $X_{max} = X_0 + YS_0$  = maximal cell concentration (mg/l),  $X_0$  = initial cell concentration (mg/l) and  $Y$  = ratio of mass of cell to mass of substrate consumed  $\left( \frac{X-X_0}{S_0-S} \right)$  (Shariful Islam et al., 2021). The ratio is the amount of cell created from 1 kg of consumed substrate; typically, 0.4-0.6 kg X/kg S. Predicted S values was determined using Equation (3).

$$S = S_0 - \frac{X-X_0}{Y} \quad (3)$$

### Monod

Half-saturation,  $K_s$  and the maximum specific growth rate,  $\mu_{max}$  are the parameters used in optimizing microbial culture. From the Monod equation that relates  $\mu$  and S, those kinetic constants can be determined by first generating  $\mu$  values using Equation (4) and (5) successively.

$$\frac{dX}{dt} = kX \left( 1 - \frac{X}{X_{max}} \right) \quad (4)$$

$$\mu = \frac{1}{X} \frac{dX}{dt} \quad (5) \text{ (Rezvani et al., 2017)}$$

$S_M$  computed from the given Monod model for Equation (6), can then be used to run appropriate Monod plots from which  $\mu_{max}/2$  corresponding with S is  $K_s$  (in mg/l) and the plateau of the hyperbola is  $\mu_{max}$ .

$$\mu = \frac{\mu_{max} S_M}{K_s + S_M} \quad (6)$$

The values of S, X,  $\mu$  and  $S_M$  are however predicted data obtained using equations and regression analysis. Table 1 shows the predicted values used in this analogy.

**Table 1. Predicted Biomass and Substrate Concentrations**

Time (hr)	X (mg/l)	S (mg/l)	Time (hr)	X (mg/l)	S (mg/l)
0	3.00E+06	900000	504	1.59E+08	510508.3
24	3.72E+06	898210.2	528	1.78E+08	461801.3
48	4.60E+06	895998.8	552	1.98E+08	412908
72	5.69E+06	893269.4	576	2.17E+08	364952.5
96	7.04E+06	889904.9	600	2.35E+08	318974.7
120	8.69E+06	885764.2	624	2.53E+08	275844.2
144	1.07E+07	880678.6	648	2.69E+08	236205.1
168	1.32E+07	874447.4	672	2.83E+08	200454.4
192	1.63E+07	866835.4	696	2.95E+08	168754.5
216	2.00E+07	857570.5	720	3.07E+08	141067.5
240	2.45E+07	846343.6	744	3.16E+08	117202.3
264	2.99E+07	832812.2	768	3.24E+08	96864.25
288	3.64E+07	816608.4	792	3.31E+08	79699.54
312	4.41E+07	797354	816	3.37E+08	65331.35
336	5.31E+07	774684.1	840	3.42E+08	53386.4
360	6.37E+07	748280.2	864	3.46E+08	43512.57
384	7.58E+07	717911.7	888	3.49E+08	35389.25
408	8.96E+07	683485	912	3.52E+08	28732.03
432	1.05E+08	645091.9	936	3.54E+08	23293.68
456	1.22E+08	603049.7	960	3.55E+08	18862.6
480	1.40E+08	557921.8			

### Generation Time

The generation time, G is the time taken for the microbial population to double; also referred to as the doubling time,  $t_d$ . It was calculated starting from X at the beginning to the end of the growth phase, because that is the period cells begin to multiply. Number of generation, n, of cells whose predicted concentrations, X were obtained from an initial value  $X_{\text{initial}} = 8247994.75$  mg/l at 192 hrs at the beginning of the exponential growth phase to  $X_{\text{final}} = 36523264.5$  mg/l at 720 hrs (end of the same phase), when  $\mu_{\text{max}} = 0.006$  hr<sup>-1</sup>,  $K_s = 4 \times 10^8$  mg/l for a material whose  $X_0 = 3 \times 10^6$  mg/l,  $S_0 = 1 \times 10^5$  mg/l and  $Y = 400$  cells/substrate, was estimated using equation 7 given by Um-e-Habiba et al. (2021).

$$n = \frac{\log X_{\text{final}} - \log X_{\text{initial}}}{\log 2} \quad (7)$$

### Approach I

G was computed by dividing t by n (i.e.  $G = \frac{t}{n}$ ). Time interval, t, implies, the change in time from the initial t = 0 to a certain t after some time. To compute G, time was numbered from 0 to 528 hrs for the logarithmic growth phase.

### Approach II

Using the expression given by Abubakar et al. (2017) as shown in Equation (8),  $\mu$  was estimated over the X values of the growth phase.

$$\mu = \frac{\ln\left(\frac{X}{X_0}\right)}{t} \quad (8)$$

The doubling time,  $t_d$  or G, was then computed using,  $t_d = \frac{\ln 2}{\mu}$ . The rate constant, k can be estimated by taking the reciprocal of G.

### Order of Reaction

Rate constant, k, was also determined using the first and zero order rate expression in terms of S at the exponential phase. Zero order is used to analyze reaction rate at high S, and is given by Equation (9).

$$S = S_0 - kt \quad (9)$$

First order is used to observe the rate of reaction at low or moderate S, as provided in Equation (10).

$$-\ln\left(\frac{S}{S_0}\right) = kt \quad (10)$$

Equation 9 and 10 were used previously by Luka et al. (2014) to determine k from substrate reduction by *Bacillus subtilis*. The hydrolysis constant,  $K_h$ , can be determined using Equation (11) based on Syaichurrozi & Rusdi (2020) and (Gallipoli et al., 2020).

$$\frac{dS}{dt} = -K_h S \quad (11)$$

## Results and Discussion

### Substrate Disappearance and Cell Proliferation

As substrate concentration decreases, microbial population increases as shown in Figure

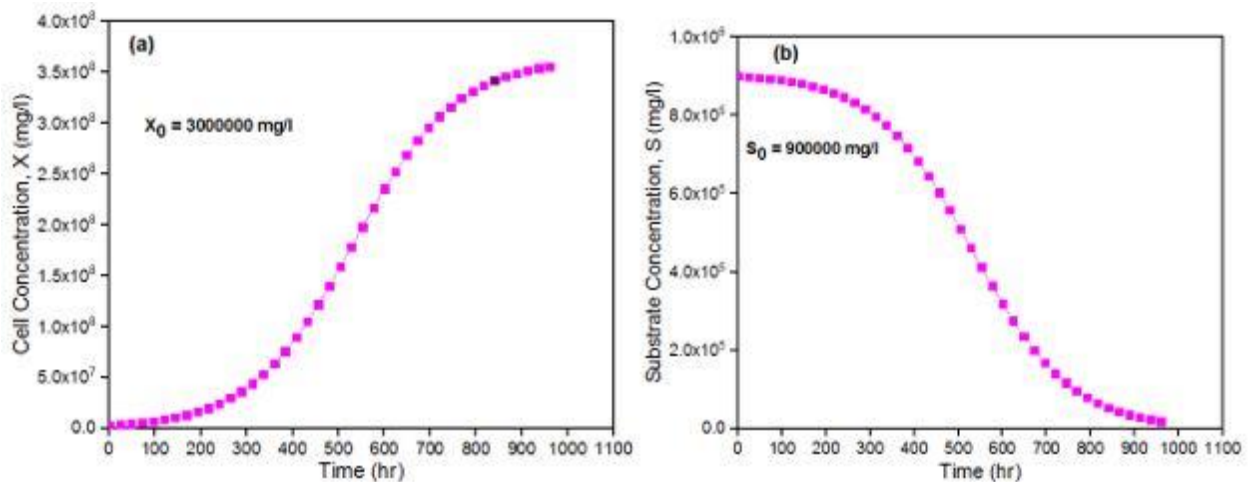


**Figure 1. S and X-Time Graph at  $\mu_{max} = 0.009\text{hr}^{-1}$  and  $K_s = 4 \times 10^8 \text{ mg/l}$**

In a certain reactor with  $X_0/S_0 = 3.33$  and  $Y (= 400)$  which is equal in both estimation using experimental and predicted S and X data, predicted values of S and X at their respective initial amount leads to the growth shown in Figure 1 and is developed following similar procedural steps followed by Liu (2017). Rate of substrate depletion and cell multiplication for the same parameters and initial conditions are both illustrated in Figure 2, where  $\frac{dS}{dt} = -\frac{\mu X}{Y}$  (Abraham, 2018) and  $\frac{dX}{dt} = \frac{\mu_{max}SX}{K_s+S}$  (Manjarres-Pinzón et al., 2021).

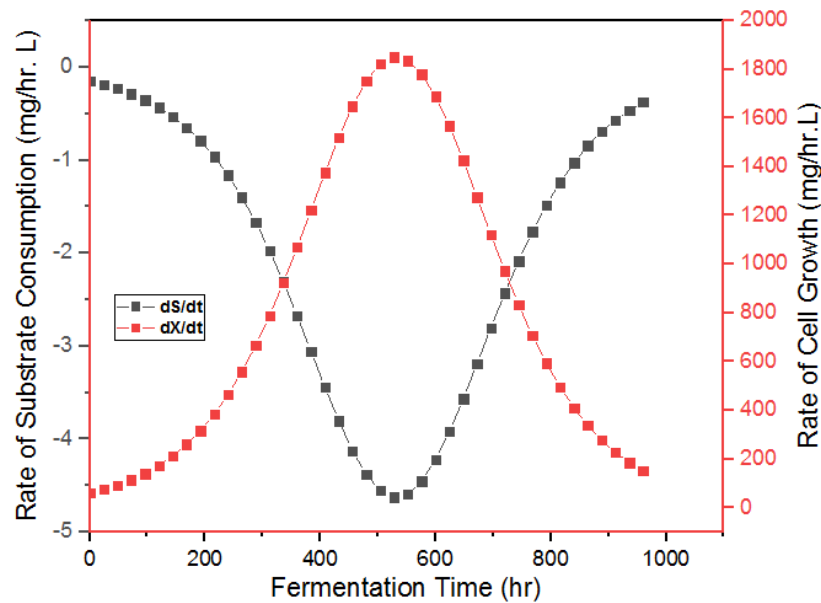


**Figure 2. Time-Relationship Between Substrate and Biomass Concentration**

What makes the ratio  $S_0 : X_0$  vital, is that it helps determine the effect of culture history on parameter estimates, as asserted by Huang (2009), who also affirmed that, when  $\frac{S_0}{X_0}$  is low, it is impossible for cells to grow in the batch assay. The author also stated that parameter correlation is strongly affected by  $\frac{S_0}{K_s}$  ratio, not  $\frac{S_0}{X_0}$ ; because by maximizing  $\frac{S_0}{K_s}$ , correlation between the Monod kinetic parameters can be minimized.

### Varying Initial Substrate Concentration

Research had been carried out to determine microbial concentration in certain organic materials as well as the concentration of the substrate such as carbohydrate in wastewater, animal residue and some lignocellulosic materials. For instance, Beltrán-prieto & Nguyen (2018) together analyzed, numerically,  $S_0$  and  $X_0$  influence on  $\mu_{max}$  using the Haldane inhibition model. Sensitivity of  $S$  when  $X$  is constant and vice versa will enable researchers to venture into materials with certain desired concentrations; example is in the production of biofertilizers and biogas, where amount of  $X$  and  $S$  is highly important. For a system with constant  $X_0 = 3 \times 10^6$  mg/l at  $\mu_{max} = 0.009 \text{ hr}^{-1}$  and  $K_s = 4 \times 10^8$  mg/l, at different initial substrate concentrations,  $S_0$ , which is  $1 \times 10^5$ ,  $3 \times 10^5$ ,  $7 \times 10^5$ ,  $9 \times 10^5$ ,  $1.1 \times 10^6$ ,  $1.3 \times 10^6$  and  $1.5 \times 10^6$  mg/l, Figure 3 shows that there is a proportional relationship with  $X$ .

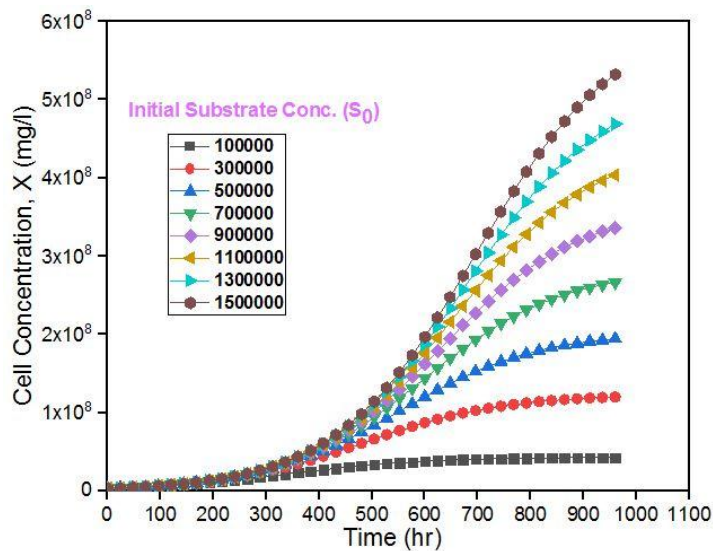


**Figure 3. Cell Concentration at Different Initial Substrate Concentration**

That is, the medium with the highest amount of initial  $S_0$ , will produce the most cells as sufficient nutrient is present for the metabolism of the organisms.  $S_0 = 1500000$  mg/l produces maximal cell density equivalent to  $5.82 \times 10^8$  mg/l while the medium with the lowest initial value,  $S_0 = 100000$  mg/l produces maximum  $X = 4.29 \times 10^7$  mg/l at the end of the process. Same with Figure 1, increase in  $X$  corresponds to a respective decrease in  $S$  from their initial values as shown in Figure 4.

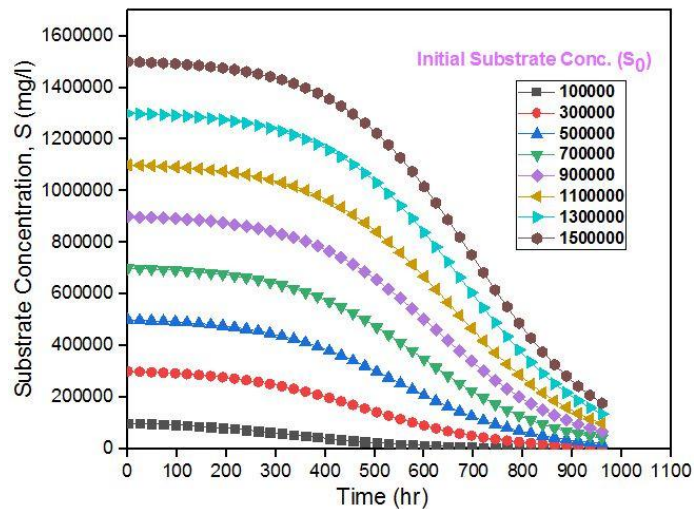


**Figure 4. Substrate Concentration from Different Initial Values**

Though, microbial growth rate will be inhibited by the substrate when  $S$  is high, increase in  $S$  imply a corresponding increase in the reaction rate, because more substrate molecules agitate and collide with enzyme molecules generated by the cells to form more product. Enzymes do not work faster even when the substrate is plentiful, so if rate of reaction requires increase, enzyme concentration should be increased not  $S$ . When amount of available  $S$  goes beyond the volume of enzyme, then breaking down of substrate automatically stops. The ratios;  $\frac{S}{S_0}$  and  $\frac{X}{X_0}$  are not significant enough to draw the attention of microbiologist to its effects on kinetics of microorganisms' growth. Clearly, since there is an inverse relationship between  $S$  and  $X$ , their plot is also similar to the ratio plots shown in Figure 5, which can be used to calculate percentage of cells produced and that of substrate remaining.

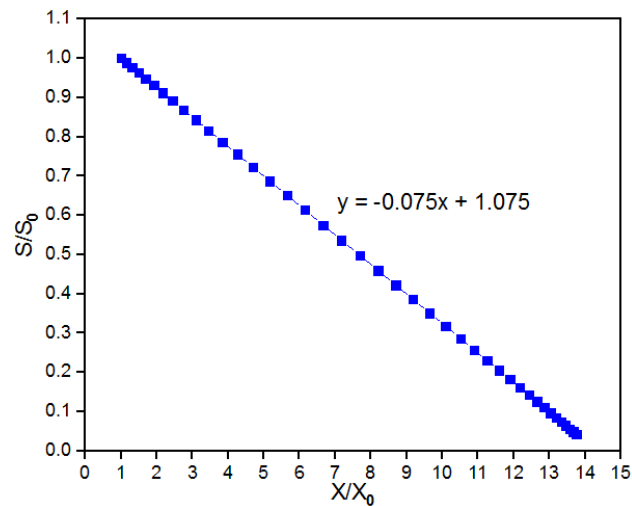
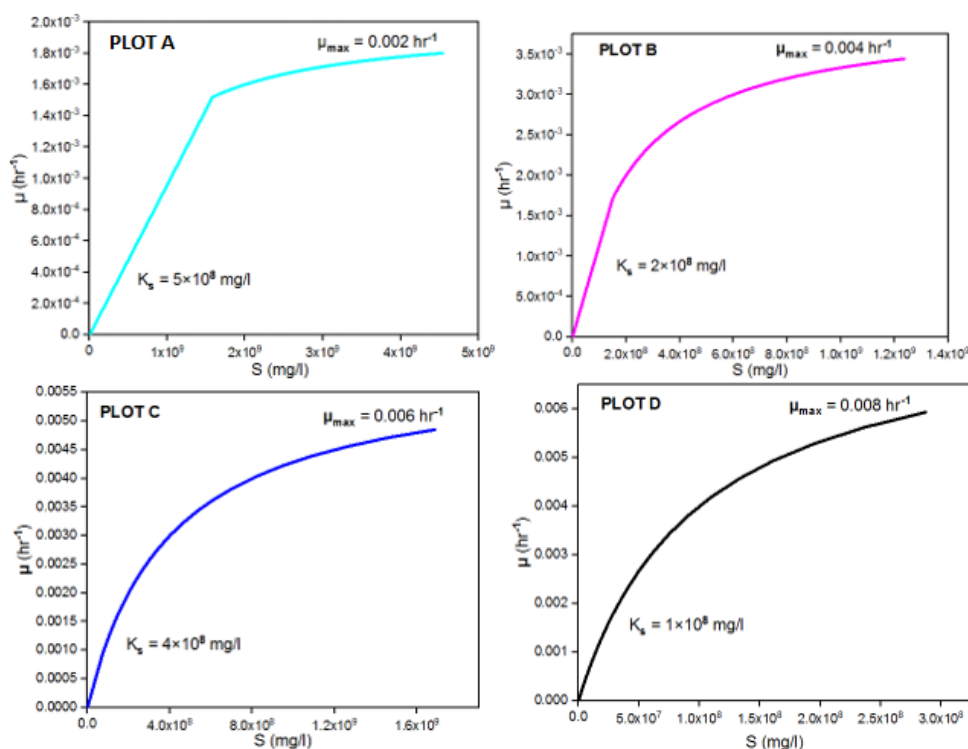


**Figure 5. Illustrating Final-to-Initial Biomass and Substrate Concentration Ratio Relationship**

The above relationship is for data of PLOT C in the next figure at  $Y = 400$ ,  $S_0 = 100000$  mg/l and  $X_0 = 3 \times 10^6$  mg/l. Also, as regards substrate concentration, its depletion can be studied especially during oil spill cleanup on land using microbes (Abubakar & Alhassan, 2021).

### Change in Kinetic Parameters

The kinetic parameters,  $\mu_{max}$  and  $K_s$  are not peculiar to Monod model alone – they are also part of several other models like the Yano & Koga inhibition model, Moser, Powell, Han and Levenspiel, Dabes, Wagman and Tseng, Luong, Andrew substrate inhibition and decay rate models, Blackman, Haldane, Heijnen and Romein and Double exponential growth kinetic models among others, which can be estimated by fitting to empirical or correlated results as explained earlier. Where  $Y = 400$ ,  $S_0 = 100000$  mg/l and  $X_0 = 3 \times 10^6$  mg/l, different combinations of  $\mu_{max}$  and  $K_s$  as shown in Figure 6 will give different  $\mu$  versus S line.



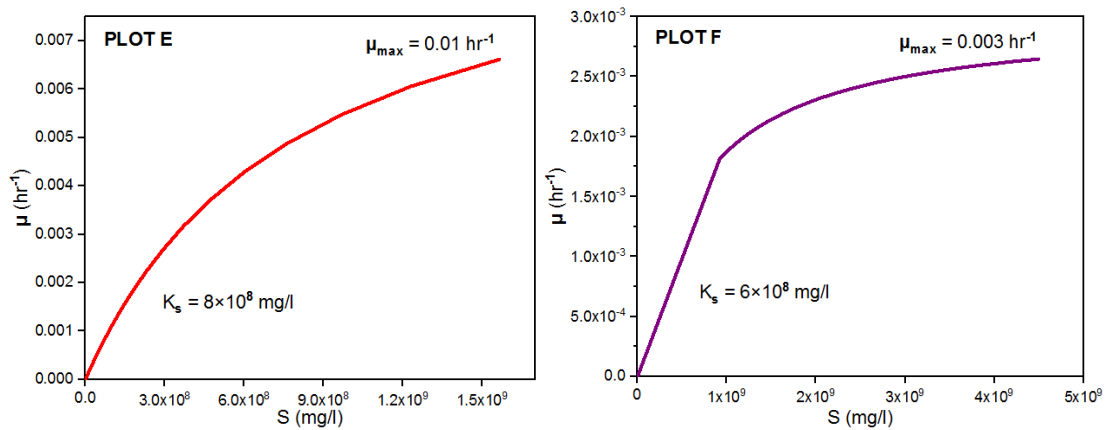


**Figure 6. Parameters from Specific Growth Rate-Time Graphs**

In the figure, an increase in  $\mu_{max}$  from  $0.002 \text{ hr}^{-1}$  in PLOT A, to  $0.003 \text{ hr}^{-1}$  in PLOT F shows a corresponding increase in  $K_s$  for the same substrate concentration. The same trend is observed moving from PLOT F-A, C-E, D-E and B-C. Exceptions are PLOT A-B, A-D, F-D and F-B indicating a decrease in the end plot values of  $K_s$ . But findings of Agarry et al. (2010) shows that as  $\mu_{max}$  decreases,  $K_s$  increase when there is jump in  $S_0$ . A higher  $K_s$  value in Monod model simply points to greater affinity to substrate. The ratio,  $\frac{S_0}{K_s}$ , had also been used previously to explain the process.

### Yield Coefficient

It was found that, when  $X_0 = 3000000 \text{ mg/l}$  and  $S_0 = 100000 \text{ mg/l}$ ,  $\mu_{max}$  increases slowly at every 100 interval of  $Y$ . An increase in  $S_0$  to  $200000 \text{ mg/l}$  at constant  $X_0$  value stated, reduces  $Y$ , whereas at constant  $S_0 = 100000 \text{ mg/l}$ , decrease in  $X_0$  result in increase in  $Y$ . Figure 7 shows that  $Y$  above 700 tends to give a constant but high  $\mu_{max}$ .

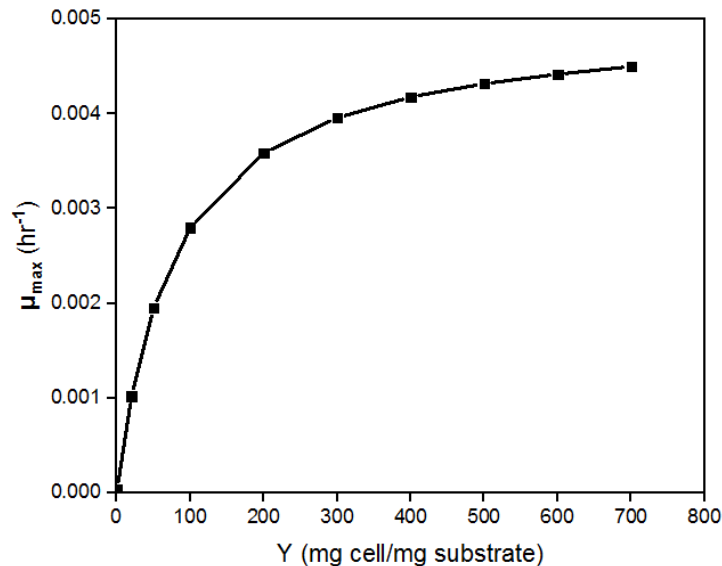


**Figure 7. Maximum Specific Growth Rate with Yield Coefficient**

From  $Y = 50$ , Figure 7 can be described as a nonlinear relationship of  $\mu_{max}$  and  $Y$  as well as in Monod plots of  $\mu$  against  $S$ . But below 50, a linear plot is obvious – same with the Monod line. Therefore high  $Y$  is synonymous with high  $\mu_{max}$  value and high  $S$  and vice versa. Also, eight models of Monod, Andrews & Noack, Haldane, Aiba, Teissier, Webb, Yano & Koga, and

Hinshelwood were used by Shariful Islam et al. (2021) to explain the  $\mu_{max}$ , Y, substrate inhibition, and  $K_s$  parameters effect on microbial growth.

### Generation Time

Time recorded from the lag phase to the death phase is shown in column 2 of Table 2, while time at the desired exponential phase, numbered from t = 0-528 hrs is the time used for the generation time computation.

**Table 2. Growth Phase Data for Finding Doubling Time and Order of Reaction**

t(hrs) [new]	t(hrs) [actual]	X(mg/l)	n	G or t <sub>d</sub> (hrs)	$\mu$ (hr <sup>-1</sup> )	k (hr <sup>-1</sup> )	S (mg/l)
0	192	8247995	1.459081	16.44871082	-	0.060795038	86880.013
24	216	9250651	1.624592	14.77293595	0.046920069	0.067691351	84373.372
48	240	10338932	1.785053	26.88996075	0.025777173	0.0371886	81652.669
72	264	11511573	1.940051	37.11243371	0.018676953	0.026945147	78721.067
96	288	12765233	2.089185	45.95092238	0.015084511	0.021762349	75586.917
120	312	14094311	2.232079	53.76154842	0.012892991	0.018600655	72264.222
144	336	15490870	2.368384	60.80095803	0.011400267	0.016447109	68772.826
168	360	16944689	2.497799	67.2592215	0.010305608	0.01486785	65138.277
192	384	18443473	2.620076	73.28031918	0.009458845	0.013646229	61391.318
216	408	19973202	2.735031	78.97533157	0.008776756	0.012662182	57566.994
240	432	21518628	2.842552	84.43118237	0.008209611	0.011843965	53703.43
264	456	23063861	2.9426	89.71658779	0.007725965	0.011146211	49840.347
288	480	24593021	3.035215	94.88620764	0.007305036	0.010538939	46017.447
312	504	26090881	3.120511	99.98361578	0.006932608	0.010001639	42272.797
336	528	27543459	3.198675	105.0434828	0.006598669	0.009519867	38641.352
360	552	28938505	3.269956	110.0932252	0.006296002	0.009083211	35153.738
384	576	30265852	3.334657	115.1542881	0.006019291	0.008684001	31835.371
408	600	31517618	3.393124	120.2431706	0.005764545	0.008316481	28705.955
432	624	32688259	3.445738	125.3722663	0.005528712	0.007976246	25779.352
456	648	33774487	3.492899	130.5505666	0.005309415	0.007659867	23063.784
480	672	34775082	3.53502	135.7842569	0.005104768	0.007364624	20562.294
504	696	35690641	3.572511	141.077227	0.004913246	0.007088316	18273.399
528	720	36523264	3.605781	146.4315093	0.004733593	0.006829131	16191.839

Final G is 146 hrs after 528 hrs, which is same using Approach I and II discussed earlier. At low X and high S, generation time is less, but increases with increase in cell numbers when S decreases from its initial value at t = 192 hrs or t = 0 hr, as illustrated in Figure 8.

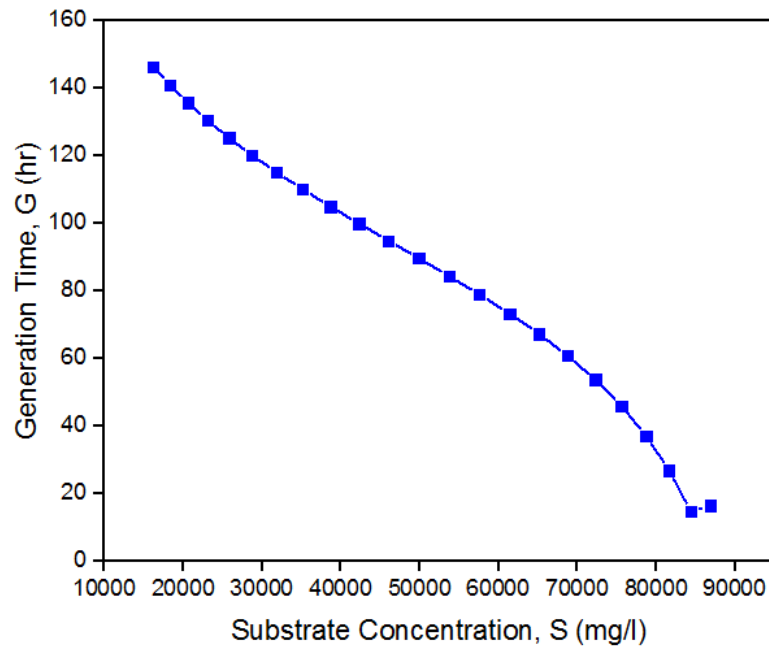


**Figure 8. Generation Time with Substrate Concentration for the Exponential Growth Phase**

The figure therefore, illustrates an inverse relationship between the generation time and the substrate concentration. At this phase, the specific growth rate decreases with increase in cell amount.

### Substrate Reduction Model

As earlier mentioned, when  $S$  is very high, the order of reaction is zero order in  $S$ , and for low  $S$ , it is 1st order in  $S$  as shown in Figure 9.

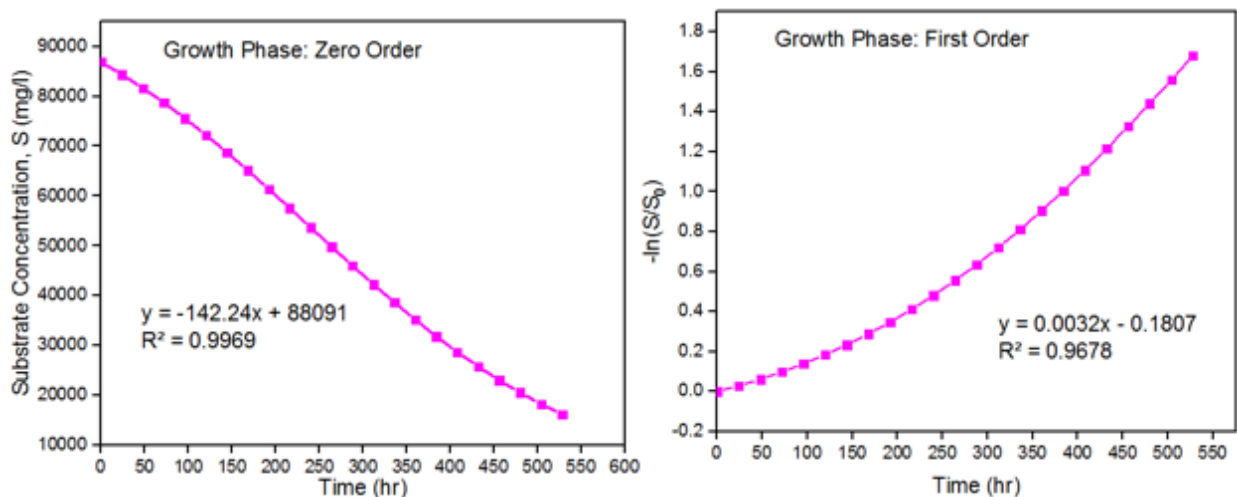


**Figure 9. Testing Zero and First Order Kinetics of Substrate Depletion**

Last column of Table 2, gives  $S_0 = 86880$  mg/l, which almost compare with the intercept of the zero order plot, 88091 mg/l. Rate constant is 142.24 mg/hr.l for zero order and 0.0032 hr<sup>-1</sup> for first order at the logarithmic growth phase. A plot of specific growth phase against substrate concentration gives PLOT C in Figure 6. In the figure, the region satisfying the zero order rate is where  $S \gg K_s$ , the one satisfying the first order description is where  $S \ll K_s$  and the whole reaction is regarded as the shifting order reaction. The constant,  $k$  can be determined at different  $\mu_{max}$  and  $K_s$  that gives PLOTS A, B, D, E and F of Figure 6, where changes in ‘ $k$ ’ at different

Monod kinetic parameters can be explained. Figure 10 relates rate of substrate consumption with the substrate concentration itself, in order to find the hydrolysis constant,  $K_h$ .

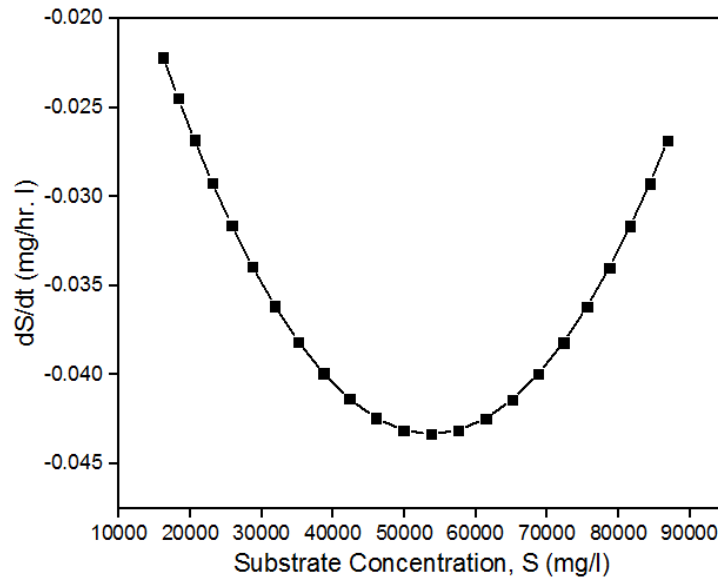


Figure 10. Finding Hydrolysis Constant

$K_h$  is difficult to determine using this procedure, but preferably, it is determined using the first order biogas kinetic model given by Ghatak & Mahanta (2014).

### Conclusion

Kinetic parameter values are hardly available for many microorganisms in nature together with substrate type. Predicted data presented in this work, covers only the range of values of X and S, from the initial to the final at time = 960 hours. Many microorganisms are capable of multiplying beyond this period. Methods of determining cell density should be carefully studied to suggest ways to improve the accuracy of data obtainable.

### Acknowledgment

The authors recognize each other's effort towards ensuring timely completion of the work.

### Conflict of Interest

There is no conflict of interest declared by the authors.

### Reference

1. Abraham, C. Study of biogas production from distillery waste water over immobilized biomass. In: Kiriamiti, K.; Ajoyi, O. (Eds.). **Moi University**. 2018.
2. Abubakar, A. M.; Alhassan, M. History, adverse effect and clean up strategies of oil spillage. **International Journal of Applied Sciences: Current and Future Research Trends (IJASCFRT)**, v. 11, no. 1, 2021. <https://doi.org/10.5281/zenodo.5557307>
3. Abubakar, B. S. U.; Abdullah, N.; Idris, A.; Zakaria, M. P.; Shokur, M. Y. Estimating the biodegradation kinetics by mixed culture degrading pyrene(pyr). **Arid Zone Journal of Engineering, Technology and Environment**, v. 13, no. 1, 2017. [www.azojete.com.ng](http://www.azojete.com.ng)
4. Agarry, S. E.; Solomon, B. O.; Audu, T. O. K. Substrate utilization and inhibition kinetics: Batch degradation of phenol by indigenous monoculture of *Pseudomonas aeruginosa*.

- International Journal for Biotechnology and Molecular Biology Research**, v. 1, no. 2, p. 22–30, 2010. <http://www.academicjournals.org/IJBMBR> ISSN
5. Beltrán-prieto, J. C.; Nguyen, L. H. N. S. Numerical analysis of initial amount of substrate and biomass in substrate inhibition process. **WSEAS Transactions on Systems and Control**, v. 13, p. 491–496, 2018.
  6. Gallipoli, A.; Braguglia, C. M.; Gianico, A.; Montecchio, D.; Pagliaccia, P. Kitchen waste valorization through a mild-temperature pretreatment to enhance biogas production and fermentability: Kinetics study in mesophilic and thermophilic regimen. **Journal of Environmental Sciences**, v. 89, p. 167–179, 2020. <https://doi.org/10.1016/j.jes.2019.10.016>
  7. Ghatak, M. Das; Mahanta, P. Comparison of kinetic models for biogas production rate from saw dust. **International Journal of Research in Engineering and Technology (IJRET)**, p. 248–254, 2014.
  8. Huang, D. The kinetics of two heterotrophic tetrachloroethene-respiring populations and their effects on the substrate interactions with Dehalococcoides strains (J. G. Becker, A. P. Davis; B. R. James; E. A. Seagren; A. Torrents (eds.)). **University of Maryland**, 2009.
  9. Liu, S. How cells grow. In: **Elsevier B. V. Bioprocess Engineering: Kinetics, Sustainability, and Reactor Design**. 2nd ed. 2017. p. pp. 629–697. <https://doi.org/10.1016/B978-0-444-63783-3.00011-3>
  10. Luka, Y.; Kefas, H. M.; Genza, J. R.; Abdul-hamid, B. A. Kinetics of bioremediation of Shinko drainage wastewater in Jimeta-Yola using Bacillus subtilis. **International Journal of Engineering Research & Technology (IJERT)**, v. 3, no. 3, p. 2429–2433, 2014. [www.ijert.org](http://www.ijert.org) 2433
  11. Manjarres-Pinzón, K.; Barrios-Ziolo, L.; Arias-Zabala, M.; Correa-Londoño, G.; & Rodríguez-Sandoval, E. Kinetic study and modeling of xylitol production using Candida tropicalis in different culture media using unstructured models. **Revista Facultad Nacional de Agronomía**, v. 74, no. 2, p. 9583–9592, 2021. <https://doi.org/https://doi.org/10.15446/rfnam.v74n2.92270>
  12. Nikitina, M. A.; Chernukha, I. M. Studying growth kinetics of microbial populations using information technology. Solving the Cauchy problem. Paper presented at BIO Web of Conferences. v. 23, p. 1–6, 2017. <https://doi.org/https://doi.org/10.1051/bioconf/20202302004>
  13. Rezvani, F.; Ardestani, F.; Najafpour, G. Growth kinetic models of five species of Lactobacilli and lactose consumption in batch submerged. **Brazilian Journal of Microbiology**, v. 48, no. 2, p. 251–258, 2017. <https://doi.org/10.1016/j.bjm.2016.12.007>
  14. Sakthiselvan, P.; Meenambiga, S. S.; Madhumathi, R. Kinetic studies of on cell growth. **IntechOpen**, 2019. <https://doi.org/http://dx.doi.org/10.5772/intechopen.84353> References
  15. Shariful Islam, M.; Kabir, K. M. A.; Tanimoto, J.; Saha, B. B. Study on Spirulina platensis growth employing non-linear analysis of biomass kinetic models. **Heliyon**, v. 7, p. 1–9, 2021. <https://doi.org/10.1016/j.heliyon.2021.e08185>

16. Syaichurrozi, I.; Rusdi, R. Development of simple kinetic model on biogas production from co-digestion of vinasse waste and tofu residue at variation of C/N Ratio. **World Chemical Engineering Journal**, v. 4, no. 1, p. 18–28, 2020. <http://jurnal.untirta.ac.id/index.php/WCEJ>
17. Um-e-Habiba; Khan, M. S.; Raza, W.; Gul, H.; Hussain, M.; Malik, B.; Azam, M.; Winter, F. A study on the reaction kinetics of anaerobic microbes using batch anaerobic sludge technique for beverage industrial wastewater. **Separations**, v. 8, no. 43, p. 1–16, 2021. <https://doi.org/https://doi.org/10.3390/separations8040043> Academic